

Transcriptomic profile of cystic fibrosis airway epithelial cells undergoing repair

Original

Transcriptomic profile of cystic fibrosis airway epithelial cells undergoing repair / Zoso, A.; Sofoluwe, A.; Bacchetta, M.; Chanson, M.. - In: SCIENTIFIC DATA. - ISSN 2052-4463. - ELETTRONICO. - 6:1(2019), p. 240. [10.1038/s41597-019-0256-6]

Availability:

This version is available at: 11583/2780652 since: 2020-01-15T15:38:23Z

Publisher:

Springer Nature

Published

DOI:10.1038/s41597-019-0256-6

Terms of use:

This article is made available under terms and conditions as specified in the corresponding bibliographic description in the repository

Publisher copyright

(Article begins on next page)

OPEN

DATA DESCRIPTOR

Transcriptomic profile of cystic fibrosis airway epithelial cells undergoing repair

Alice Zoso, Aderonke Sofoluwe , Marc Bacchetta & Marc Chanson *

Pathological remodeling of the airway epithelium is commonly observed in Cystic Fibrosis (CF). The different cell types that constitute the airway epithelium are regenerated upon injury to restore integrity and maintenance of the epithelium barrier function. The molecular signature of tissue repair in CF airway epithelial cells has, however, not well been investigated in primary cultures. We therefore collected RNA-seq data from well-differentiated primary cultures of bronchial human airway epithelial cells (HAECs) of CF (F508del/F508del) and non-CF (NCF) origins before and after mechanical wounding, exposed or not to flagellin. We identified the expression changes with time of repair of genes, the products of which are markers of the different cell types that constitute the airway epithelium (basal, suprabasal, intermediate, secretory, goblet and ciliated cells as well as ionocytes). Researchers in the CF field may benefit from this transcriptomic profile, which covers the initial steps of wound repair and revealed differences in this process between CF and NCF cultures.

Background & Summary

In this study, we compared by next generation RNA-sequencing (RNA-seq) the transcriptomic profile of human airway epithelial cells from cystic fibrosis (CF) patients and healthy donors (NCF). F508del, the most common variant of the CF transmembrane conductance regulator (*CFTR*) gene, is associated with a severe clinical phenotype that leads to chronic inflammation and infection of the airways by opportunistic pathogens, including *Pseudomonas aeruginosa*¹. The continuous exposure to severe harmful stimuli places lungs at constant risk of injury and thereby, tissue repair is crucial for maintaining lung homeostasis^{2,3}. *CFTR* plays a key role in regeneration of the airway epithelium, the repair of which is obviously insufficient to maintain lung functions in CF^{4–10}. Knowledge of the molecular mechanisms regulating airway epithelial cell differentiation was mostly gained from lineage tracing studies in mouse models³. Less is known in human although application of single-cell RNA-seq on airway biopsies and primary HAEC cultures are rapidly filling up this gap^{11–13}. The present work aims to identify gene expression changes in CF and NCF human airway epithelial cells (HAECs) undergoing repair. Some cultures of NCF and CF HAECs were also exposed to flagellin for 24 h to mimic *Pseudomonas aeruginosa* infection and processed for RNA-seq.

The tracheobronchial airway epithelium is pseudostratified and constituted of basal (BCs), secretory Club/Clara (SCs), ionocytes (ICs), mucin-producing goblet (GCs) and ciliated cells (CCs)^{3,11,12,14}. It is well demonstrated that epithelium regeneration/repair is initiated by BC proliferation to repopulate the denuded injured area³. In parallel, subsets of progenitor cells (suprabasal cells, sBCs) cycle and/or progressively mature to intermediate - or early progenitor - cells leading to the generation of SCs. After wound closure, all cells exit the cell cycle, BCs return to their original state while SCs terminate their differentiation to GCs and CCs. Figure 1 illustrates the logFC changes in expression of markers of the different cell subtypes with time of repair after injury of CF and NCF HAEC primary cultures. We focused on the initial steps of repair by comparing the post-wounding conditions (24 h post-wounding pW, wound closure WC, usually reached 42 hours after injury, and 2-days post wound closure pWC) to the control non-wounded condition (NW). We monitored TP63, cytokeratin 5 (KRT5) and KRT14 for BCs (Fig. 1a), KRT4 and KRT13 for sBCs (Fig. 1b), SCGB1A1 and SCGB3A1 for SCs (Fig. 1c), MUC5B and SPDEF for GCs (Fig. 1d), FOXJ1, FOXI1 and *CFTR* for CCs and ICs (Fig. 1e). Globally, proliferation can be evaluated by the expression of MKI67 (Fig. 1b) and early differentiation by the expression of KRT8 (Fig. 1d), a marker which is not detected in BCs and sBCs. Note that FUT4, a marker of immature SCs is detected

Departments of Pediatrics, Gynecology & Obstetrics and of Cell Physiology & Metabolism, Geneva University Hospitals and Medical School of the University of Geneva, Geneva, Switzerland. *email: marc.chanson@unige.ch

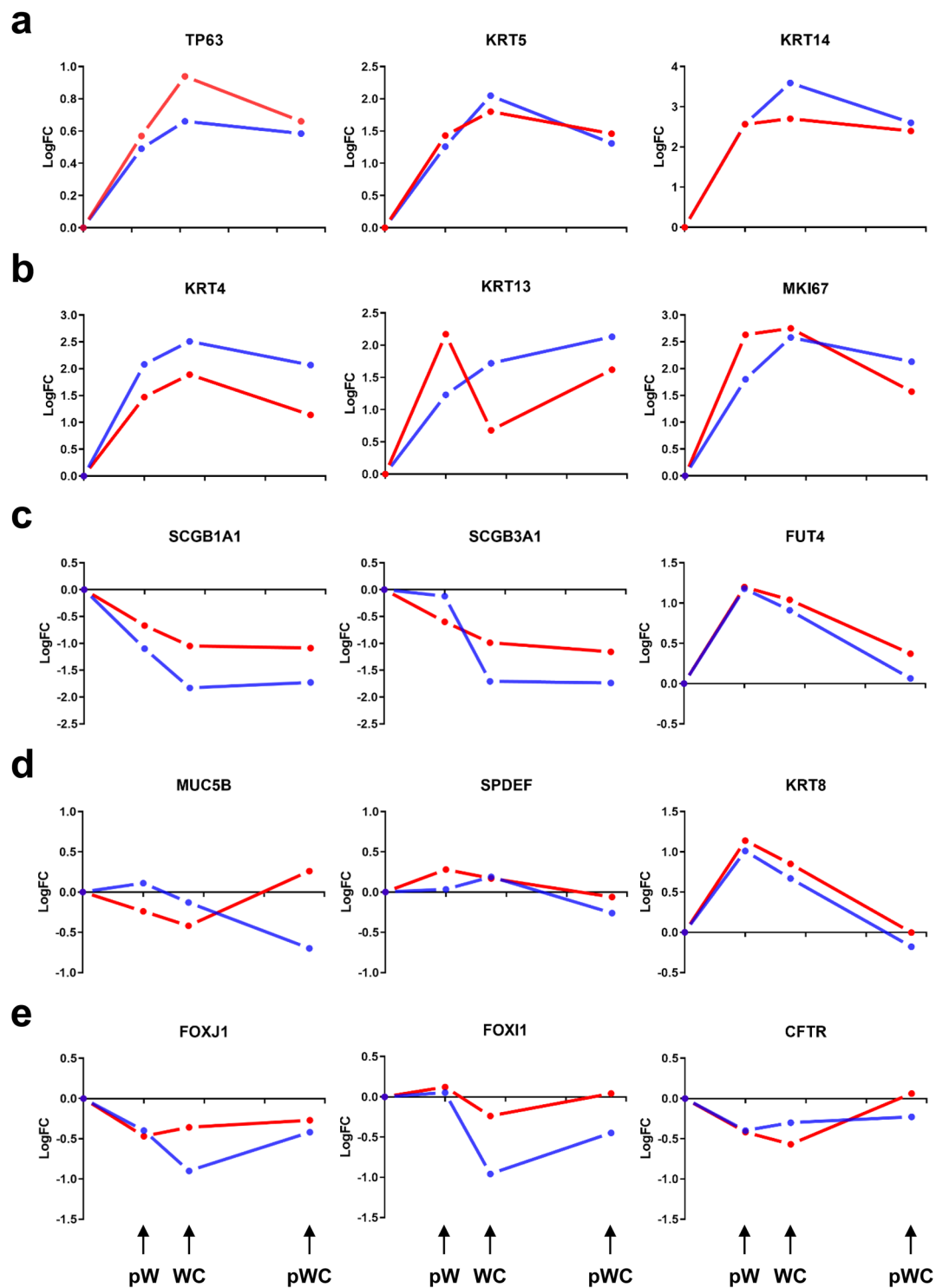


Fig. 1 Changes in gene expression (logFC) of markers of subpopulations of NCF (blue lines and dots) and CF (red lines and dots) HAECs at different times of wound repair as compared to their initial expression (values set at 0) in non-wounded conditions. **(a)** Expression levels of basal cell marker genes: TP63, KRT5 and KRT14. **(b)** Expression levels of suprabasal cell marker genes (KRT4 and KRT13) and of a marker of cell proliferation (MKI67). **(c)** Expression levels of Club cell marker genes (SCGB1A1 and SCGB3A1), including the marker of immature cells (FUT4). **(d)** Expression levels of goblet cell marker genes (MUC5B and SPDEF) and of KRT8, which is a marker of early cell differentiation. **(e)** Expression levels of ciliated cell and ionocyte marker genes (FOXJ1 and FOXI1, respectively), with both subpopulations expressing CFTR. Data are expressed as means; error bars were not drawn for clarity since no statistical differences were observed between NCF and CF cultures. pW: post wounding; WC: wound closure; pWC: post wound closure.

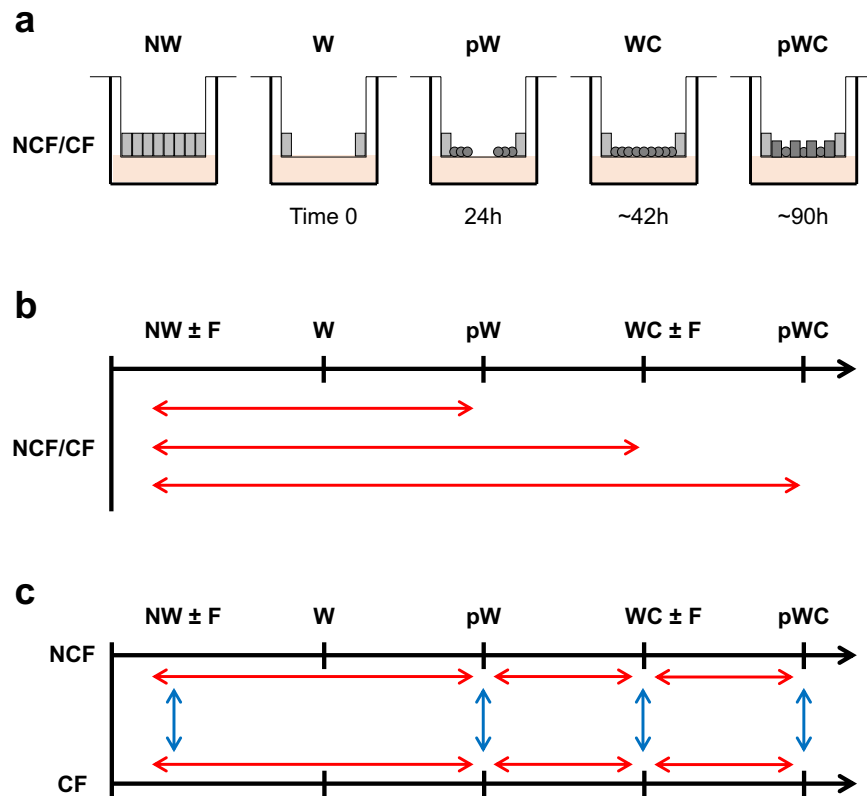


Fig. 2 Experimental design and conditions comparison. **(a)** Schematic illustration of the wound-induced repair process in HAECs. Well-differentiated airway epithelium 3D cultures from CF patients and NCF donors were used, corresponding the non-wounded (NW) condition. At time 0, a circular wound (W) was induced in the center of the culture but leaving intact the epithelium at the periphery. Twenty-four hours after wounding (pW), migrating and proliferating cells started to cover the denuded area. Wound closure (WC) was reached 42 hours after wounding. mRNA was isolated from two Transwells per patient/donor and for each condition, NW, pW, WC and 48 hours after wound closure (pWC; 90 hours after wounding). In parallel experiments, 2 NW and WC Transwells per patient/donor were treated with flagellin to mimic infection with *Pseudomonas aeruginosa*. **(b)** Illustration of the gene expression comparisons performed between different conditions after wounding (pW, WC, pWC) and the initial NW condition, exposed or not to flagellin (F). **(c)** Illustration of the gene expression comparisons performed for all conditions between CF and NCF cultures.

(Fig. 1c). The results indicate that the repair process is engaged after wounding in both CF and NCF cultures and that our RNA-seq allows monitoring gene expression during the initial steps before the generation of mature SCs. A schematic overview of the experimental conditions as well as the comparisons performed between conditions and groups are provided in Fig. 2. Table 1 indicates the number of gene changes for each time point after wounding relative to the NW conditions (top). Comparison of the number of gene changes between conditions (pW vs NW; WC vs pW; pWC vs WC) is also given (middle). We also performed comparison of gene changes between CF and NCF HAEC cultures for the different conditions (bottom). Again, up- and downregulated genes in CF HAECs are detected for all conditions, suggesting alterations in the switch between proliferation and differentiation for CF HAECs. Finally, flagellin stimulation at Time 0 (NW) and at WC further highlighted differences in the transcriptomic response of CF HAECs (Table 2).

In summary, this study presents RNA-seq data from healthy and CF human HAECs undergoing repair after injury. We extracted gene expression of typical marker genes of the different cell subtypes that constitute the airway epithelium and report differences in the repair process between CF and NCF cultures. We believe that these data will be valuable for researchers studying airway epithelium regeneration in the context of the CF disease.

Methods

Cell cultures. Well-differentiated primary cultures of bronchial airway epithelial cells (MucilAir™ and MucilAir™-CF) on Transwell filters at the air-liquid interface for 45–60 days were purchased from Epithelix Sàrl (Plan-les-Ouates, Switzerland). All CF HAEC cultures were generated from 7 patients homozygous for the F508del CFTR variant. NCF cultures were generated from 7 subjects but one culture (subject 4) did not differentiate appropriately and was discarded. Detailed characteristics of the patients (age, sex, smoking status) are not available. The basal medium, which consisted of DMEM:F12 (3:1, Life Technologies, Zug, Switzerland) supplemented with 1.5% Ultrosor G (Bioserpa, Cergy, France) and antibiotics, was refreshed every 2 days. Mechanical wounding was performed using an airbrush linked to a pressure regulator, as previously described¹⁵.

	# up-regulated genes	# down-regulated genes	No change	# with FC 2	of which # FC < 2	of which # FC > 2
Compare different Times per Group						
NCF						
pW vs NW	2930	2359	9669	1260	339	921
WC vs NW	3871	3459	7628	2148	791	1357
pWC vs NW	630	127	14201	305	15	290
CF						
pW vs NW	3297	3142	8519	1244	360	884
WC vs NW	3109	2881	8968	1136	266	870
pWC vs NW	474	58	14426	195	3	192
Compare different Conditions per group						
NCF						
pW vs NW	2930	2359	9669	1260	339	921
WC vs pW	57	15	14886	32	2	30
pWC vs WC	517	1414	13027	410	358	52
CF						
pW vs NW	3297	3142	8519	1244	360	884
WC vs pW	0	0	14958	0	0	0
pWC vs WC	212	668	14078	141	107	34
Compare different Groups per Condition						
CF vs NCF						
NW	181	110	14667	162	40	122
pW	47	86	14825	95	73	22
WC	217	480	14261	309	241	68
pWC	55	114	14789	111	80	31

Table 1. Number of differently expressed genes with FDR (False Discovery Rate) 5% and the number of which have a fold-change 2 (FC 2) thresholds. (Top) Comparisons between different times of HAEC repair with initial, non-wounded condition, for NCF and CF cultures. (Middle) Comparisons between different times of HAEC repair for NCF and CF cultures. (Bottom) Comparisons between NCF and CF cultures for the different times of HAEC repair. NW, non-wounded; pW, 24 h post-wound; WC, wound closure; pWC, 2d post-wound closure.

	# up-regulated genes	# down-regulated genes	No change	# with FC 2	of which # FC < 2	of which # FC > 2
Compare different Times per Group						
NCF + F						
WC vs NW	1292	624	14082	656	122	534
CF + F						
WC vs NW	1302	668	14028	647	142	505
Compare different Conditions per group						
NCF ± F						
NW	643	70	15285	496	35	461
WC	31	14	15953	37	13	24
CF ± F						
NW	564	189	15245	438	83	355
WC	222	34	15742	183	21	162
Compare different Groups per Condition						
CF + F vs NCF + F						
NW	14	140	15844	144	135	9
WC	9	38	15951	43	38	5

Table 2. Number of differently expressed genes with FDR (False Discovery Rate) 5% and the number of which have a fold-change 2 (FC 2) thresholds. (Top) Comparisons between wound closure (WC) of HAEC repair and the initial, non-wounded (NW) condition, for NCF and CF cultures treated with flagellin (F). (Middle) Comparisons between flagellin (F)-treated and non-treated NCF and CF cultures that were not wounded (NW) and at time of wound closure (WC) of HAEC repair. (Bottom) Comparisons between NCF and CF non-wounded (NW) cultures and time of wound closure (WC) of HAEC repair after flagellin (F) exposure.

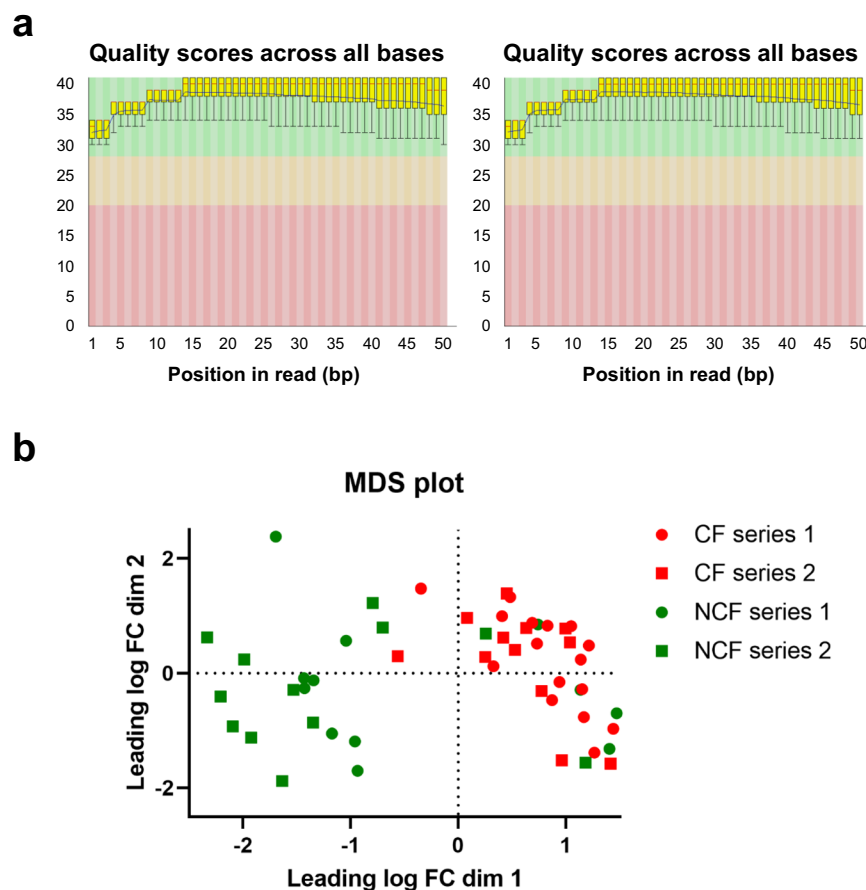


Fig. 3 Quality assessment FASTQ data. (a) The quality distribution along the reads plot is shown for one NCF (left, sample 54) and one CF (right, sample 26) sample. Box and whisker plots demonstrate the distribution of per base quality for each left and right read position read for each of the analyzed samples. Mean value is indicated by the dark line; the yellow box represents the interquartile range (25–75%) with the lower and upper whiskers representing the 10 and 90% points, respectively. (b) MDS (principal components analysis) plot indicating the similarity of the counts in the samples obtained from the first (black letters) and the second (red letters) series of NCF and CF cultures.

RNA extraction. Total RNA was extracted using Qiagen RNeasy Kit (Qiagen, Hombrechtikon, Switzerland), according to the manufacturer's instructions. At 24 hours post-wound (pW) and at WC, the Transwell filters were cut off and undamaged cells at the periphery of the wound were discarded from the repairing cells using a sterile scalpel before lysis and RNA extraction. Two filters were pooled per condition. RNA-seq was performed by the iGE3 Genomic Platform at the Faculty of medicine, University of Geneva.

Differential gene expression analysis. Library size normalizations and differential gene expression calculations have been performed using the package edgeR (<http://www.ncbi.nlm.nih.gov/pmc/articles/PMC2796818/>). The genes having a count above one count per million reads (cpm) in at least 3 samples were kept for the analysis. For each comparison, the latest condition was used as the 'control', i.e. genes with a positive fold-change are more expressed in the first condition compared to the 'control' condition. Genes with maximal expression value in any of the compared conditions lower than 1 RPKM (reads per kb per million read) were removed from the analysis before calling for differentially expressed genes. The differentially expressed gene tests were done with a general linear model with a negative binomial distribution. The differentially expressed genes p-values are corrected for multiple testing error with a 5% FDR (false discovery rate) and the correction used is Benjamini-Hochberg (BH). By default, the fold-change (FC) and the Benjamini-Hochberg corrected p-value thresholds were set to 2 and 0.01, respectively. Genes with higher Benjamini-Hochberg corrected p-value or lower FC were not considered as differentially expressed.

Data Records

The data can be accessed to NCBI Gene Expression Omnibus (GEO) with the accession number GSE127696¹⁶. The lists of differentially expressed genes with FDR 5% and FC 2 thresholds for the comparisons indicated in Tables 1 and 2 are available in figshare¹⁷. Datasets of original reads for all conditions (NCF and CF, before and after wounding) are available in the NCBI SRA repository¹⁸.

Technical Validation

RNA integrity assessment. Before sequencing, QuBit (Invitrogen) was used to assess RNA quality and quantity without prior purification of the samples.

RNA-seq data quality assessment. Single read of 50 bases, TruSeq stranded mRNA, was performed with a HiSeq 4000 from Illumina. The sequencing quality control was done with FastQC (<http://www.bioinformatics.babraham.ac.uk/projects/fastqc/>). Quality scores of 32–40 were achieved (Fig. 3a), corresponding to 1/1000 and 1/10'000 chance of errors, respectively. The reads were mapped with STAR, an ultra-fast and universal RNA-seq aligner, which can do spliced alignments and read clipping: <http://bioinformatics.oxfordjournals.org/content/early/2012/10/25/bioinformatics.bts635>.

Only the reads that are mapped once to the genome are considered for the read allocation to genomic features. Ambiguous reads were removed using featureCounts: <http://www.ncbi.nlm.nih.gov/pubmed/24227677>.

Reads mapping is provided as a Supplementary Data File (Online-only Table 1). For polyA-enriched RNAseq, 70% or more reads uniquely assigned to a gene are considered really good, although this percentage may be affected by the nature of the different expressed genes.

Sequencing was performed on two different occasions with RNA samples collected at one-year interval times. Figure 3b shows the multi-dimensional scaling (MDS) plot (principal components analysis) of the samples, which gives an indication of the similarity of the counts in the earlier and former experiments (first and second series, respectively). No batch effect could be observed between the two sequenced data.

Received: 25 June 2019; Accepted: 20 September 2019;

Published online: 29 October 2019

References

- Cohen, T. S. & Prince, A. Cystic fibrosis: a mucosal immunodeficiency syndrome. *Nat. Med.* **18**, 509–519 (2012).
- Puchelle, E., Zahm, J. M., Tournier, J. M. & Coraux, C. Airway epithelial repair, regeneration, and remodeling after injury in chronic obstructive pulmonary disease. *Proc. Am. Thorac. Soc.* **3**, 726–733 (2006).
- Wansleben, C., Barkauskas, C. E., Rock, J. R. & Hogan, B. M. Stem cells of the adult lung: their development and role in homeostasis, regeneration, and disease. *Wiley Interdiscip. Rev. Dev. Biol.* **2**, 131–148 (2013).
- Voynow, J. A., Fischer, B. M., Roberts, B. C. & Proia, A. D. Basal-like cells constitute the proliferating cell population in cystic fibrosis airways. *Am. J. Respir. Crit. Care Med.* **172**, 1013–1018 (2005).
- Hajj, R. *et al.* Human airway surface epithelial regeneration is delayed and abnormal in cystic fibrosis. *J. Pathol.* **211**, 340–350 (2007).
- Schiller, K. R., Maniak, P. J. & O'Grady, S. M. Cystic fibrosis transmembrane conductance regulator is involved in airway epithelial wound repair. *Am. J. Physiol. Cell Physiol.* **299**, C912–C921 (2010).
- Trinh, N. T. *et al.* Improvement of defective cystic fibrosis airway epithelial wound repair after CFTR rescue. *Eur. Respir. J.* **40**, 1390–1400 (2012).
- Crespin, S. *et al.* Cx26 regulates proliferation of repairing basal airway epithelial cells. *Int. J. Biochem. Cell Biol.* **52**, 152–160 (2014).
- Itokazu, Y. *et al.* Reduced GM1 ganglioside in CFTR-deficient human airway cells results in decreased β 1-integrin signaling and delayed wound repair. *Am. J. Physiol. Cell Physiol.* **306**, C819–C830 (2014).
- Adam, D. *et al.* CFTR rescue with VX-809 and VX-770 favors the repair of primary airway epithelial cell cultures from patients with class II variants in the presence of *Pseudomonas aeruginosa* exoproducts. *J. Cyst. Fibros.* **17**, 705–714 (2018).
- Treutlein, B. *et al.* Reconstructing lineage hierarchies of the distal lung epithelium using single-cell RNA-seq. *Nature* **15**, 371–375 (2014).
- Plasschaert, L. W. *et al.* A single-cell atlas of the airway epithelium reveals the CFTR-rich pulmonary ionocyte. *Nature* **560**, 377–381 (2018).
- Revinski, D. R. *et al.* CDC20B is required for deuterosome-mediated centriole production in multiciliated cells. *Nat. Commun.* **7**, 4668 (2018).
- Whitsett, J. A. & Alenghat, T. Respiratory epithelial cells orchestrate pulmonary innate immunity. *Nat. Immunol.* **16**, 27–35 (2015).
- Crespin, S. *et al.* Approaches to study differentiation and repair of human airway epithelial cells. *Methods Mol. Biol.* **742**, 173–185 (2011).
- Gene Expression Omnibus*, <https://identifiers.org/geo/GSE127696> (2019).
- Zoso, A., Sofoluwe, A., Bacchetta, M. & Chanson, M. Transcriptomic profile of cystic fibrosis airway epithelial cells undergoing repair. <https://doi.org/10.6084/m9.figshare.c.4638233> (2019).
- NCBI Sequence Read Archive*, <https://identifiers.org/ncbi/insdc.sra:SRP187187> (2019).

Acknowledgements

This work was supported by grants from ABCF2, CFCH and the Swiss National Science Foundations to M.C. We would like to thank Natacha Civic and Mylène Docquier at the iGE3 Genomics platform (Faculty of medicine, University of Geneva), Sylvain Lemeille (Dept. of pathology and immunology, Faculty of medicine, University of Geneva) for the bioinformatics and Joanna Bou Saab for early RNA sample collection.

Author contributions

A.Z. analyzed the data. A.S. prepared samples and analyzed the data. M.B. performed the wound injury and monitored the cell cultures. M.C. wrote the Data Descriptor, and analyzed the data.

Competing interests

The authors declare no competing interests.

Additional information

Correspondence and requests for materials should be addressed to M.C.

Reprints and permissions information is available at www.nature.com/reprints.

Publisher's note Springer Nature remains neutral with regard to jurisdictional claims in published maps and institutional affiliations.



Open Access This article is licensed under a Creative Commons Attribution 4.0 International License, which permits use, sharing, adaptation, distribution and reproduction in any medium or format, as long as you give appropriate credit to the original author(s) and the source, provide a link to the Creative Commons license, and indicate if changes were made. The images or other third party material in this article are included in the article's Creative Commons license, unless indicated otherwise in a credit line to the material. If material is not included in the article's Creative Commons license and your intended use is not permitted by statutory regulation or exceeds the permitted use, you will need to obtain permission directly from the copyright holder. To view a copy of this license, visit <http://creativecommons.org/licenses/by/4.0/>.

The Creative Commons Public Domain Dedication waiver <http://creativecommons.org/publicdomain/zero/1.0/> applies to the metadata files associated with this article.

© The Author(s) 2019